

CORRESPONDENCE

Open Access

Efficient and precise generation of Tay–Sachs disease model in rabbit by prime editing system

Yuqiang Qian¹, Ding Zhao¹, Tingting Sui¹, Mao Chen¹, Zhiquan Liu¹, Hongmei Liu¹, Tao Zhang¹, Siyu Chen¹, Liangxue Lai^{1,2} and Zhanjun Li¹

Dear Editor,

Tay–Sachs disease (TSD) is a progressive neurodegenerative disorder due to an autosomal recessively inherited deficiency of β -hexosaminidase A (HexA)¹. The four-bases (TATC) insertion in exon 11 of the *HEXA* (*HEXA* ins TATC) accounts for 80% of Tay–Sachs disease from the Ashkenazi Jewish population². However, no typical clinical phenotypes, such as neurological abnormalities, the restricted pattern of distribution of GM2-ganglioside and membranous cytoplasmic bodies in the brain, were observed in *HEXA*^{-/-} mouse models, due to the difference in the ganglioside degradation pathways in mice and human³. Thus, it is desired to generate an ideal animal model to accurately mimic *HEXA* ins TATC in TSD patients. CRISPR–Cas9 system-mediated HDR⁴ has been used to generate the mutation of *HEXA* ins TATC, however, low efficiency and high indels impede its application.

Recently Anzalone et al.⁵ described a “search-and-replace” genome editing technology named prime editing (PE) that mediates 12 possible base-to-base conversions, without requiring DSBs or donor DNA templates in human cells. In addition, a previous study showed that, compared to mice, the late onset of TSD in adult rabbits⁶ shared more similarities with human regarding physiology, anatomy, and genetics⁷. Thus, we generated a novel TSD rabbit model using the PE system, and characterized

the typical phenotype of muscle weakness, ataxia, and mental disorders in the *HEXA* ins TATC rabbit model.

We first validated the editing efficiencies of PEs (PE2, PE3, PE3b) in HEK293FT cells at fifteen loci: five loci for base insertion, eight loci for base substitutions, and two loci for base deletion (Supplementary Table S1). Sanger sequencing results showed that the base insertion at a frequency from 4% to 22% (Fig. 1a and Supplementary Fig. S2), the base substitutions at a frequency from 4% to 36%, and the base deletion at a frequency from 7% to 12% were determined using PEs (Supplementary Figs. S1 and S2), respectively. These results indicate that PEs were effective in generating base insertion, substitution, and deletion in HEK293FT cells.

Next, we tested the efficiency of the PE system in rabbit embryos at three gene loci of *HEXA*, *HBB*, and *TYR*, which are associated with clinical diseases in ClinVar data⁸ (Supplementary Table S2). Sanger sequencing results showed that 9 of 20 desired *HEXA* ins TATC were determined using PE2 with the efficiency of 4.1%–15.4%, while the efficiency is 8%–37.5% using PE3. In addition, 1 of 14 desired *HBB* with an efficiency of 10% and 1 of 10 desired *TYR* with an efficiency of 14% were generated using PE3, while there is no desired mutation was detected for these two sites using PE2 (Fig. 1b and Supplementary Fig. S3).

We then targeted the *HEXA* ins TATC to test the efficiency of the PegRNA PBS length (8–16 nt) and RT template length (10–18 nt) in rabbit embryos. TIDE analyzing⁹ revealed significantly higher editing efficiencies by using PegRNA with 12 nt PBS and 14 nt RT template (Fig. 1c, d and Supplementary Table S3). Additionally, the significantly increased undesired indels were determined by using CRISPR–Cas9 system-mediated HDR (Fig. 1e and Supplementary Tables S3, S8), which is consistent with the previous study⁴. Thus, PE3 with 12 nt PBS and

Correspondence: Liangxue Lai (lai_liangxue@gibh.ac.cn) or Zhanjun Li (lizj_1998@jlu.edu.cn)

¹Key Laboratory of Zoonosis Research, Ministry of Education, College of Animal Science, Jilin University, Changchun, Jilin, China

²CAS Key Laboratory of Regenerative Biology, Guangdong Provincial Key Laboratory of Stem Cell and Regenerative Medicine, South China Institute for Stem Cell Biology and Regenerative Medicine, Guangzhou Institutes of Biomedicine and Health, Chinese Academy of Sciences, Guangzhou, Guangdong, China

These authors contributed equally: Yuqiang Qian, Ding Zhao, Tingting Sui

© The Author(s) 2021



Open Access This article is licensed under a Creative Commons Attribution 4.0 International License, which permits use, sharing, adaptation, distribution and reproduction in any medium or format, as long as you give appropriate credit to the original author(s) and the source, provide a link to the Creative Commons license, and indicate if changes were made. The images or other third party material in this article are included in the article's Creative Commons license, unless indicated otherwise in a credit line to the material. If material is not included in the article's Creative Commons license and your intended use is not permitted by statutory regulation or exceeds the permitted use, you will need to obtain permission directly from the copyright holder. To view a copy of this license, visit <http://creativecommons.org/licenses/by/4.0/>.

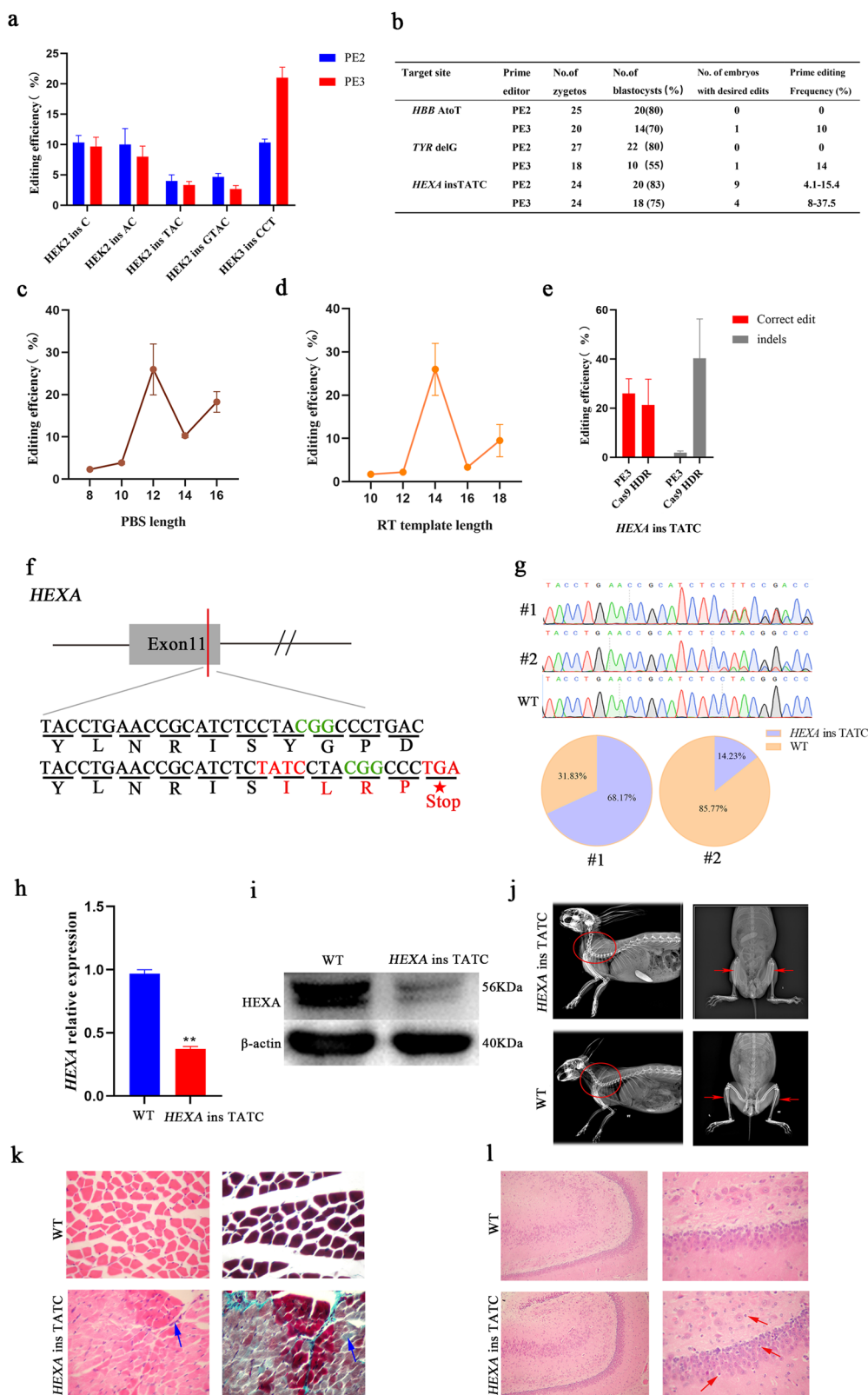


Fig. 1 (See legend on next page.)

(see figure on previous page)

Fig. 1 PE induced efficient and precise gene editing in rabbit. **a** The base insertion efficiency of PE system in HEK293FT cells. **b** PE induced efficient and precise gene editing in rabbit embryos. **c** Editing frequency (*HEXA* ins TATC) of PegRNA screening with PBS length (8–16 nt) in rabbit embryos. **d** Editing frequency (*HEXA* ins TATC) of PegRNA screening with RT template length (10–18 nt) in rabbit embryos. **e** Editing frequency (*HEXA* ins TATC) of CRISPR–Cas9 system-mediated HDR compare with PE3. **f** The target sequence at *HEXA* locus by PE system. The PAM and sgRNA target sequences are shown in green and black, target mutation (red), frameshift mutation leads to PTC mutation (red and red star). **g** Editing frequency determination of *HEXA* ins TATC rabbit by deep sequencing. **h** Expression of *HEXA* gene was determined by qRT-PCR. **i** *HEXA* protein was determined by western blot. **j** X-ray radiography of WT and *HEXA* ins TATC rabbits. Red circle, increased cervical lordosis; Red arrows, clamping of the limbs. **k** Masson's trichrome staining of gastrocnemius from WT and *HEXA* ins TATC rabbits. Blue arrow highlights the myopathy with fibrosis and inflammatory cell infiltration. **l** HE staining of hippocampus from WT and *HEXA* heterozygous rabbits. The red arrow highlights the enlargement of perineural space.

14 nt RT template was used for the generation of *HEXA* ins TATC rabbits in the following study.

The *HEXA* ins TATC introduces a premature termination codon (PTC) in exon 11, which leads to deficient activity of the hexosaminidase A (HexA)¹⁰ (Fig. 1f). In this study, 2 of 4 *HEXA* ins TATC rabbits were determined using Sanger sequencing and targeted deep sequencing, with the 68.17% and 14.23% mutation efficiency for #1 and #2 pups, respectively (Fig. 1g). Furthermore, no sgRNA sequence-dependent off-target mutations in *HEXA* ins TATC rabbits were found by deep sequencing (Supplementary Fig. S4a, b), suggesting the accuracy of PE system-mediated *HEXA* ins TATC mutations in rabbits.

Furthermore, the heritability of *HEXA* ins TATC in rabbits was determined by Sanger sequencing (Supplementary Fig. S5), qRT-PCR (Fig. 1h), and western blot (Fig. 1i). The results showed a significantly reduced *HEXA* in *HEXA* ins TATC rabbits compared with WT controls. The typical phenotypes of the increasingly frequent of head raising, convulsions (Supplementary Fig. S6a and Movies S1, S2), abnormal gait with decreased sway length (Supplementary Fig. S6b and Movies S1, S2), clamping of the limbs, and increased cervical lordosis (Fig. 1j), muscle fibrosis (Fig. 1k) and enlargement of perineural space (Fig. 1l) were also determined in *HEXA* ins TATC rabbits when compared with WT controls. These phenotypes were similar with late-onset or chronic adult gangliosidosis in TSD patient exhibiting as limb-girdle weakness, followed by the development of ataxia and progressive neuromuscular weakness¹¹.

In summary, this study for the first time verified the feasibility of PE system-mediated base insertions, deletions, and conversions in rabbit. This ideal and novel *HEXA* ins TATC rabbit model would be beneficial for the pathogenic mechanism study and drug screening to treat TSD in the future.

Acknowledgements

We thank Peiran Hu and Nannan Li for assistance at the Embryo Engineering Center for critical technical assistance. This study was financially supported by the National Key Research and Development Program of China Stem Cell and

Translational Research (2019YFA0110700). The Strategic Priority Research Program of the Chinese Academy of Sciences (XDA16030501, XDA16030503), Key Research & Development Program of Guangzhou Regenerative Medicine, and Health Guangdong Laboratory (2018GZR110104004).

Author contributions

Y.Q., L.L., and Z.Li. conceived and designed the experiments. Y.Q., D.Z., and T.Z. performed the experiments. Z.Liu., M.C., S.C. and Y.Q. analyzed the data. M.C., H.L., and T.S. contributed reagents/materials/analysis tools. Y.Q. and D.Z. wrote the paper. All authors have read and approved the final manuscript.

Conflict of interest

The authors declare no competing interests.

Publisher's note

Springer Nature remains neutral with regard to jurisdictional claims in published maps and institutional affiliations.

Supplementary information The online version contains supplementary material available at <https://doi.org/10.1038/s41421-021-00276-z>.

Received: 25 November 2020 Accepted: 22 April 2021

Published online: 06 July 2021

References

- Kolodny, E. H. Molecular genetics of the beta-hexosaminidase isoenzymes: an introduction. *Adv. Genet.* **44**, 101–126 (2001).
- Frisch, A. et al. Origin and spread of the 1278insTATC mutation causing Tay-Sachs disease in Ashkenazi Jews: genetic drift as a robust and parsimonious hypothesis. *Hum. Genet.* **114**, 366–376 (2004).
- Phaneuf, D. et al. Dramatically different phenotypes in mouse models of human Tay-Sachs and Sandhoff diseases. *Hum. Mol. Genet.* **5**, 1–14 (1996).
- Jasin, M. & Haber, J. E. The democratization of gene editing: Insights from site-specific cleavage and double-strand break repair. *DNA Repair* **44**, 6–16 (2016).
- Anzalone, A. V. et al. Search-and-replace genome editing without double-strand breaks or donor DNA. *Nature* **576**, 149–157 (2019).
- Rickmeyer, T. et al. GM2 gangliosidosis in an adult pet rabbit. *J. Comp. Pathol.* **148**, 243–247 (2013).
- Wang, Y. et al. Generation of knockout rabbits using transcription activator-like effector nucleases. *Cell Regen.* **3**, 3 (2014).
- Landrum, M. J. et al. ClinVar: public archive of interpretations of clinically relevant variants. *Nucleic Acids Res.* **44**, D862–D868 (2016).
- Brinkman, E. K., Chen, T., Amendola, M. & van Steensel, B. Easy quantitative assessment of genome editing by sequence trace decomposition. *Nucleic Acids Res.* **42**, e168 (2014).
- Myerowitz, R. & Costigan, F. C. The major defect in Ashkenazi Jews with Tay-Sachs disease is an insertion in the gene for the alpha-chain of beta-hexosaminidase. *J. Biol. Chem.* **263**, 18587–18589 (1988).
- Jeyakumar, M. et al. An inducible mouse model of late onset Tay-Sachs disease. *Neurobiol. Dis.* **10**, 201–210 (2002).